International Journal on Magnetic Particle Imaging
Vol 8, No 1, Suppl 1, Article ID 2203085, 4 Pages

Infinite Science Publishing

Proceedings Article

MPI region of interest (ROI) analysis and quantification of iron in different volumes

O. C. Sehl[a,*] · B. Tiret[b] · M. A. Berih[a] · A. V. Makela[c] · P. W. Goodwill[b] · P. J. Foster[a]

[a] Robarts Research Intitute, Western University, London, Canada
[b] Magnetic Insight Inc., Alameda, USA
[c] The Institute for Quantitative Health Science & Engineering, Michigan State University, East Lansing, USA
*Corresponding author, email: osehl@uwo.ca

Abstract

MPI directly detects superparamagnetic iron oxides (SPIOs), which should enable precise, accurate and linear quantification. However, selecting a region of interest (ROI) has strong effects on MPI quantification results. Ideally, ROI selection should be simple, user-independent, and widely applicable. In this work, we describe and compare four MPI ROI selection methods and assesses their performance *in vitro* and *in vivo*. To explore the effect of ROI selection, ten ferucarbotran phantoms were imaged, each contained the same amount of iron but varied in volume. Three users tested the accuracy of the ROI methods for quantification of these samples. Lastly, quantification of ferucarbotran-labeled stem cells *in vivo* was demonstrated with the four ROI methods. We demonstrate that each ROI method has strengths. We conclude there is an important trade-off between ROI size and the accuracy of iron quantification, therefore the choice of ROI selection method for each study must be carefully informed.

I. Introduction

Magnetic particle imaging (MPI) quantification of superparamagnetic iron oxide nanoparticles (SPIO) provides unique opportunities in tracking cell therapies [1], imaging inflammation [2], and magnetic hyperthermia [3]. *In vivo*, SPIOs can be dispersed in larger volumes (e.g. a tumor, 1 cm^3) whereas MPI quantification is conducted using calibration samples, of known amounts of iron, typically in small volumes (~10 µL). Thus, careful and rigorous choice of the region of interest (ROI) is essential for quantification. Our development of MPI cell tracking techniques has identified a demand for standardized, reproducible, and accurate quantification methods for MPI. In this work, we first develop four unique ROI selection methods and assess their linearity of quantitation using *in vitro* ferucarbotran phantoms. We then evaluate the inter-user reproducibility. Last, we apply these methods to quantify an *in vivo* ferucarbotran-labeled mesenchymal stem cell (MSC) transplant.

II. Material and methods

Ten ferucarbotran samples (VivoTrax™, Magnetic Insight Inc.) were prepared in conical tubes, each containing 34.4 µg iron mixed with increasing volumes of saline, from 6.25 µL (Sample 1) to 1.2 mL (Sample 10). Each sample was imaged separately using a MOMENTUM™ MPI system (Magnetic Insight Inc.) in 2D with a 5.7 T/m selection field gradient and drive field strengths of 20 mT and 26 mT, in the X and Z axes, respectively.

II.I. ROI analysis methods

The ten 2D images were analyzed using four ROI selection methods: **(1)** An ROI was drawn at $pixelvalue > c \cdot s_{max}$, where c is a scaling factor < 1 and $s_{max}(A.U./mm^2)$ is the maximum value for the signal of interest. We used $c = 0.5$. **(2)** A line profile was drawn through the maximum value of the signal of interest and the distance between the two points of

maximum curvature was estimated (Δx). This spatial distance was used to define a circular ROI with diameter $d = c\Delta x$, we used $c = 2$ as the scaling factor. **(3)** All images were quantified with the same circular ROI with diameter $d = c \cdot \Delta x_{max}$, where Δx_{max} is the largest ROI diameter in the dataset from method 2. **(4)** The standard deviation of system noise (SD) was measured by imaging an empty sample holder. A mask was generated that selected pixels with $pixelvalue > c \cdot SD$. We used $c = 5$ to select signals, according to the Rose Criterion [4].

II.II. Signal calibration

A series of calibration samples containing known amounts of ferucarbotran (0.34 – 55 µg Fe in 10 µL) were imaged with one sample per image. Each of methods 1-4 were used to create a calibration curve and convert the MPI signal measured from samples 1-10 into an estimate of iron mass using linear regression.

II.III. Inter-user reproducibility

The ROI analysis (part II.I) was repeated by 2 additional users on the same set of images. The absolute inter-user variability was calculated as the standard error of measurement (SEM):

$$SEM = SD(value1, value2, value3). \quad (1)$$

The coefficient of variation (CoV), representing the relative interobserver variability was calculated as:

$$CoV(\%) = \frac{SEM}{(Average(value1, value2, value3))} \cdot 100. \quad (2)$$

When the users' measurements are in perfect correspondence, SEM and CoV are equal to 0 [5].

II.IV. ROI selection for *in vivo* quantification

$1 \cdot 10^5$ labeled mesenchymal stem cells were administered to NSG mice by subcutaneous or intraperitoneal injection [6]. Isotropic 2D images were acquired before and immediately after injection using a 3.0 T/m selection field gradient and drive field strength of 22 mT and 26 mT in the X and Z axes, respectively. Signal calibration (Part II.II) was repeated with these parameters, then quantification of *in vivo* images was conducted using the four ROI methods.

III. Results and discussion

The four methods for ROI selection are demonstrated for images of *in vitro* samples of ferucarbotran in Fig. 1.

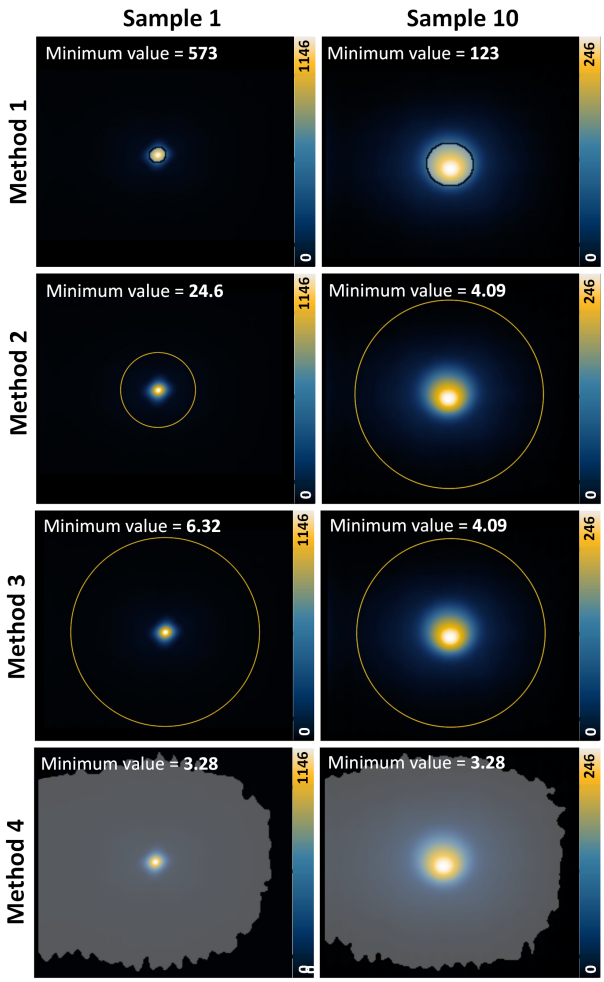

Figure 1: A demonstration of ROI methods 1, 2, 3, and 4 on two samples of ferucarbotran (Samples 1 and 10).

III.I. Quantification of *in vitro* samples

MPI of samples 1-10 are shown in Fig. 2A. As the fixed mass of ferucarbotran is diluted with increasing amounts of saline, the peak signal diminishes and the width broadens. Quantification of iron mass in ferucarbotran Samples 1-10 are shown in Fig 2B and C. Method 1 and 2 were accurate in quantifying the iron mass for samples in low volumes, which were similar to that of calibration samples (10 µL). However, as the ferucarbotran sample is diluted, Method 1 and 2 overestimate iron mass by up to 70% (Sample 10) and this pattern persists with different threshold factors (c = 0.1, 0.5, and 0.7). Methods 3 and 4 use larger ROIs and adequately capture the broader extents of the MPI signal. This leads to more accurate (<5% error) estimation of iron mass, regardless of the sample volume. Method 4 maintained accuracy when thresholding with larger multiples of the noise SD (c = 5, 10, and 25), however increasing c will eventually compromise quantification.

10.18416/ijmpi.2022.2203085

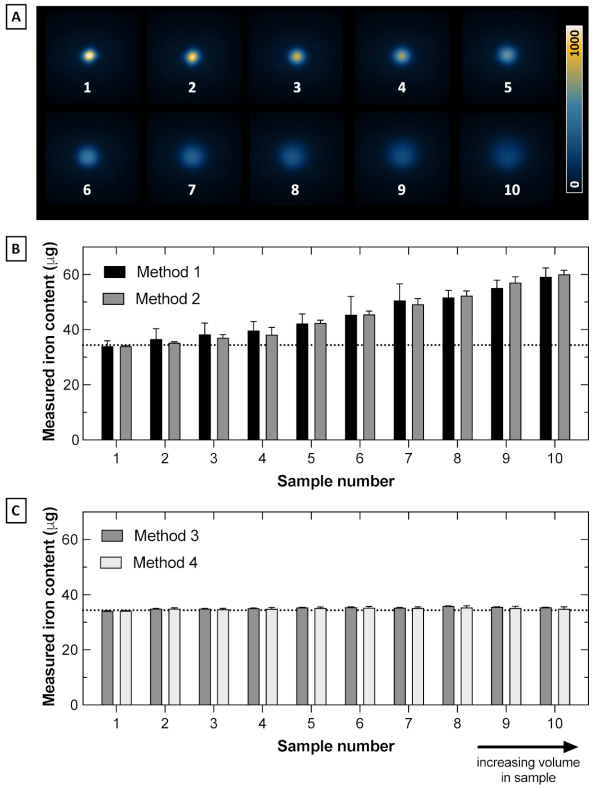

Figure 2: A. Projection images of ten samples of 34.4 µg ferucarbotran, in increasing volumes of saline (Samples 1-10). Images are displayed using the same window/level. B and C. Measurements of iron content from samples 1-10 were performed by 3 users, using methods 1-4. The dotted line represents the true amount of iron (34.4 µg).

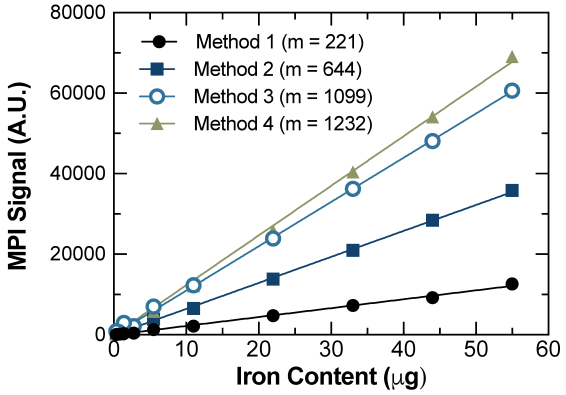

Figure 3: MPI signal calibration relates MPI signal measured from known amounts of iron. This was performed for all four ROI methods. The slope (m) of these lines was used to calculate iron mass from MPI signal measured from Samples 1-10.

Table 1: Comparison of ROI methods 1-4, in terms of ROI size, time spent, user variability, the ability to form custom-shaped ROIs and accuracy of quantification for iron in differing volume.

Criteria / Method	1	2	3	4
Size of ROI	Small	Med	Large	Large
Speed	Med	Slow	Med	Fast
User variability	Med	High	Med	Low
Custom shapes	Yes	No	No	Yes
Accuracy with volume	Poor	Poor	Good	Good

III.II. Signal calibration

A strong linear relationship ($R2 > 0.998$) was found between ferucarbotran mass (0.34 – 55 µg Fe) and MPI signal, using the four methods of ROI selection (Fig. 3).

III.III. Inter-user reproducibility

The SEM and CoV for each ROI selection method were as follows: 1.389, 3.02 % (Method 1); 3.770, 8.49 % (Method 2); 0.433, 1.23 % (Method 3); and 0.061, 0.17 % (Method 4). These parameters indicate method 4 had the smallest inter-user variability and method 2 had the largest differences between users.

III.IV. ROI selection for *in vivo* quantification

The application of the four ROI selection methods for quantification of ferucarbotran-labeled cells *in vivo* is demonstrated in Fig. 4. Background signal associated with iron in the mouse digestive system, present prior to the injection of cells [1], challenges this analysis (Fig. 4A).

For quantification of iron-labeled cells administered by subcutaneous (point) injection (Fig. 4B), Method 1 forms a small ROI around signal at the site of injection, with a custom shape. Method 2 ROI is larger than 1 and includes some, but not all, of the background signal, leading to inaccurate quantification. Method 3 and 4 use large ROIs which include signal both from cells and background. To isolate signal associated with the cells, the net signal was calculated (subtraction of pre-injection signal from post-injection). For this point injection, methods 1, 3, and 4 lead to similar quantification results (Fig. 4D).

The signal associated with iron-labeled cells administered by intraperitoneal (disperse) injection co-localizes with background signal (Fig. 4C). The calculation of net signal using ROI selection methods 1 and 2 led to inaccurate results because the delineation is inconsistent pre- and post- injection of cells. For example, for method 1 the background signal is delineated at $0.5 \cdot s_{max} = 4.2$ whereas for post-injection, $0.5 \cdot s_{max} = 6.2$. Methods 3 and 4 allow for consistent delineation, with quantification similar to the cells administered subcutaneously (Fig. 4D).

10.18416/ijmpi.2022.2203085

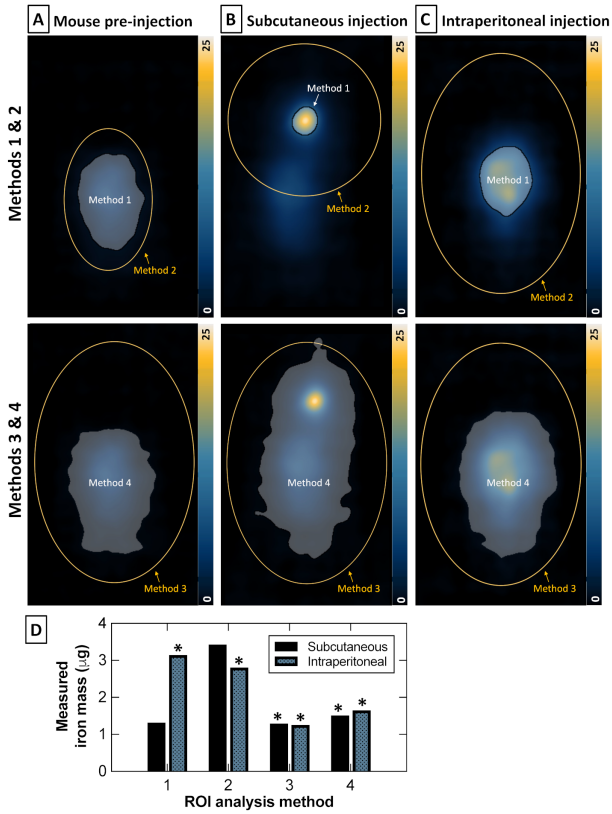

Figure 4: A. Demonstration of *in vivo* quantification using methods 1-4 on mice which received 100,000 ferucarbotran-labeled stem cells by subcutaneous or intraperitoneal injection. *In vivo* background signal was also measured. B. Iron mass measured from *in vivo* images. The asterisks indicate net iron content was calculated (difference in pre- vs. post-injection).

IV. Conclusions

Each of these four ROI selection methods have advantages, and no single method meets all desired criteria (Table 1). Method 1 generates a small ROI, which helps to achieve separation of multiple adjacent signals present in a single image. However, in the phantom study, all three users estimated less accurately and precisely using this method, particularly for dilute samples of iron. Method 2 aims to include more of the MPI point spread function, however the quantitative accuracy for dilute ferucarbotran phantoms did not improve. Ultimately, these first two methods are best suited for high-SNR and high-resolution signals, from samples in a similar volume, and break down for more complex images. Since method 2 requires 3-user inputs per image, it is the most time consuming, laborious, and the greatest inter-user variability was observed. Method 3 uses fixed dimensions on all images in a dataset thus it is optimal for datasets that assume the same physical layout of objects and can be used for quantification across a large SNR range. Method 4 threshold-based segmentation has many advantages, including simplicity, quick analysis, and high reproducibility. With methods 3 and 4, all three users estimate iron mass accurately and precisely for *in vivo* phantoms and return consistent quantification of iron-labeled cells *in vivo*. Smaller ROIs are possible, if different values of c are chosen. Our hope is these ROI selection methods will be widely adopted by MPI users to improve the accuracy and consistency of iron quantification.

Acknowledgments

Research reported in this publication was supported by Natural Sciences and Engineering Research Council of Canada (NSERC) and NCI of the National Institutes of Health under award number R43CA233155.

Author's statement

Authors state no conflict of interest.

References

[1] O. C. Sehl et al., A perspective on cell tracking with magnetic particle imaging, Tomography, vol. 6, no. 4, pp. 315-324, 2020.

[2] P. Chandrasekharan et al., Non-radioactive and sensitive tracking of neutrophils towards inflammation using antibody functionalized magnetic particle imaging tracers, Nanotheranostics, vol. 5, no. 2, pp. 240-255, 2021.

[3] Z. W. Tay et al., Magnetic particle imaging-guided heating in vivo using gradient fields for arbitrary localization of magnetic hyperthermia therapy, ACS Nano, vol. 12, pp. 3699-3713, 2018.

[4] A. Rose, The sensitivity performance of the human eye on an absolute scale, Journal of the Optical Society of America, vol. 38, no. 2, pp. 196-208 (1948).

[5] Y. W. S. Jauw et al., Interobserver reproducibility of tumor uptake quantification with 89Zr-immunoPET: a multicenter analysis, European Journal of Nuclear Medicine and Molecular Imaging, vol. 46, no. 9, pp. 1840-1849, 2019.

[6] O. C. Sehl & P. J. Foster, The sensitivity of magnetic particle imaging and fluorine-19 magnetic resonance imaging for cell tracking, Sci Rep, vol. 11, no. 1, pp. 1-12, 2021.

